Maternal and Zygotic Expression of a *nanos*-Class Gene in the Leech *Helobdella robusta*: Primordial Germ Cells Arise from Segmental Mesoderm

Dongmin Kang,* **Marc Pilon,†** **and David A. Weisblat‡,[1]**

*Department of Biological Sciences, Stanford University, Stanford, California 94305-5020;
†Lundberg Laboratory, Chalmers University, Göteborg, Sweden ‡Department of Molecular and
Cell Biology, 385 LSA, University of California, Berkeley, California 94720-3200*

The *nanos*-class gene of the leech *Helobdella robusta* (*Hro-nos*) is present as a maternal transcript whose levels decay during cleavage; HRO-NOS protein is more abundant in the D quadrant cells relative to the A, B, and C quadrants; and HRO-NOS is more abundant in the ectodermal precursor cell (DNOPQ) than in its sister mesodermal precursor (DM) (Pilon and Weisblat, 1997). Here, using in situ hybridization, we show that *Hro-nos* mRNA is broadly distributed throughout the zygote, is concentrated in both animal and vegetal teloplasm during stage 1 and is at higher levels in DNOPQ than in DM at stage 4b. *Hro-nos* expression increases after stage 7, as judged by *in situ* hybridization, developmental RT-PCR, and western blots; this increase must therefore represent later zygotic expression. Of particular interest, during stages 9 and 10, each of 11 mid-body segments (M8-M18) has a pair of *Hro-nos* positive "spots" comprising of one or two large cells each. These spots later disappear in an anteroposterior progression. We find that these *Hro-nos*-expressing cells are of mesodermal origin, arising in a segmentally iterated manner from the M lineage, and correspond to cells previously proposed as primordial germ cells (PGCs; Bürger, 1891; Weisblat and Shankland, 1985). These results support the proposal that *nanos*-class genes functioned in the specification of germline cells in the ancestral bilaterian and possibly in a separate process related to embryonic polarity in the ancestral protostome. © 2002 Elsevier Science (USA)

*Key Words:* annelid; leech; *Helobdella*; germline; *nanos*.

INTRODUCTION

In *Drosophila,* the gene *nanos* (*nos*) encodes a zinc-finger protein that serves two distinct embryological functions, establishing A-P polarity and specifying germline precursor cells. In contrast to initial conclusions (Gavis and Lehmann, 1992; Wang *et al.,* 1994), maternal *nos* transcripts are only weakly localized at the posterior pole (Bersten and Gavis, 1999), but translation is tightly restricted to the posterior pole, setting up a nonuniform distribution of NOS protein along the A-P axis (Bersten and Gavis, 1999; Irish *et al.,* 1989). NOS and PUMILIO cooperate to repress the translation of maternal *hunchback* RNA in the posterior part of the embryo, and thereby initiate the determination of abdominal cell fates (Irish *et al.,* 1989; Murata and

Wharton, 1995; Parisi and Lin, 2000). With respect to the germline, *nanos* function is required for proper development of primordial germ cells (PGCs) and viability of germline stem cells (Forbes and Lehmann, 1998; Kobayashi *et al.,* 1996). More recently, it has been reported that NOS acts as a downregulator of mitosis and transcription during the development of the germline (Deshpande *et al.,* 1999).

Questions as to which aspect(s) of *nos* function are conserved among *nanos*-class genes in other organisms are of interest both for deducing the nature of ancestral animals and for understanding the evolution of developmental mechanisms between the three main groups of bilaterally symmetric animals. To date, *nos*-class genes have been reported for the toad *Xenopus laevis* and zebrafish *Danio rerio* [both deuterostomes; *Xcat-2* (Mosquera *et al.,* 1993) and *nanos1* (Köprunner *et al.,* 2001), respectively], the leech *Helobdella robusta* (a lophotrochozoan; *Hro-nos*; Pilon and Weisblat, 1997), the nematode *Caenorhabditis elegans* (like
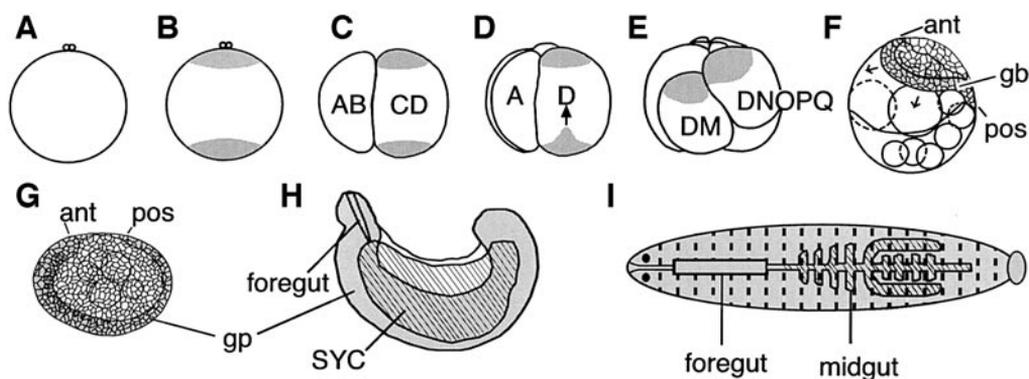
FIG. 1. Schematic depiction of relevant stages of *Helobdella* development. Panels A-H show lateral views with animal pole at top and (prospective) anterior to left; panel I shows a dorsal view. (A) Stage 1 embryo before teloplasm formation (2 hours AZD); polar bodies are indicated at animal pole. (B) Stage 1 embryo after teloplasm (shading) has formed at animal and vegetal poles (3 hours AZD). (C) Stage 2 (4 h AZD); teloplasm is inherited by cell CD at first cleavage. (D) Stage 3 (6 h AZD); arrow indicates the movement of vegetal teloplasm toward the animal pole. (E) Stage 4b (9 h AZD); cells DNOPQ and DM each inherits teloplasm at third cleavage. (F) Early stage 8 (~61 h AZD); DM and DNOPQ have cleaved to generate the full complement of 10 teloblasts (circles, only 8 are shown in the drawing) plus additional micromeres. Each teloblast produces a column of segmental founder cells (blast cells); ipsilateral bandlets merge, forming left and right germinal bands (gb; shading; only left gb is visible in this lateral view), which are covered by micromere-derived epithelium. As blast cells are added to their posterior (pos) ends, the germinal bands elongate and move ventrovegetally (arrows) and coalesce from anterior (ant) to posterior (pos) along the ventral midline, forming the germinal plate (gp), accompanied by the expansion of the micromere-derived epithelium. (G) Late stage 8 (~94 h AZD): the completed germinal plate (shading) extends from anterior to posterior, defining the ventral territory of the embryo. (H) Mid stage 10 (~155 h AZD); during stage 10, segmental tissues arise from the proliferation and differentiation of cells within the germinal plate (shading), the edges of which gradually expand dorsolaterally and meet at the dorsal midline, closing the definitive body tube. Macromeres, teloblasts and supernumerary blast cells have fused into a syncytial yolk cell (SYC; hatching), from which the midgut will arise; foregut arises largely from micromere progeny. (I) Stage 11 (~185 h AZD); during this stage gut segmentation is completed, the yolk in the gut is exhausted and the juvenile leech is ready for its first meal.
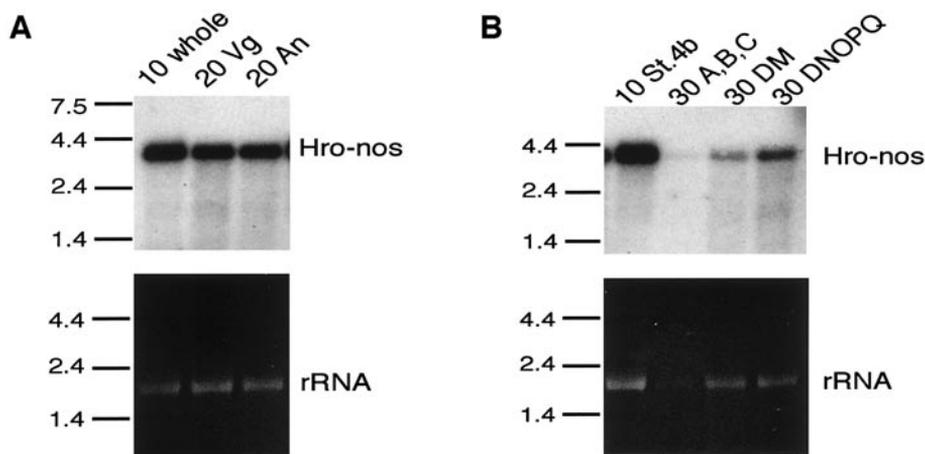
FIG. 2. Distribution and segregation of *Hro-nos* transcripts in early development, analyzed by Northern blot analysis of dissected embryos. For each panel, size markers (kb) are indicated at left, rRNA is shown in the ethidium-stained gel as a loading control. (A) Northern blot comparison of 10 intact stage 1 embryos (lane 1), with 20 vegetal and 20 animal halves (lanes 2 and 3, respectively) shows that *Hro-nos* transcripts are distributed uniformly between the animal and vegetal halves of the zygote. (B) Comparison of 10 intact stage 4b embryos (lane 1) with 30 macromeres, 30 DM cells and 30 DNOPQ cells (lanes 2–4, respectively) shows that *Hro-nos* transcripts segregate with teloplasm (represented by rRNA) to cells DM and DNOPQ at this stage, and are relatively more abundant in ectodermal precursor cell (DNOPQ) than in mesodermal precursor cell (DM).
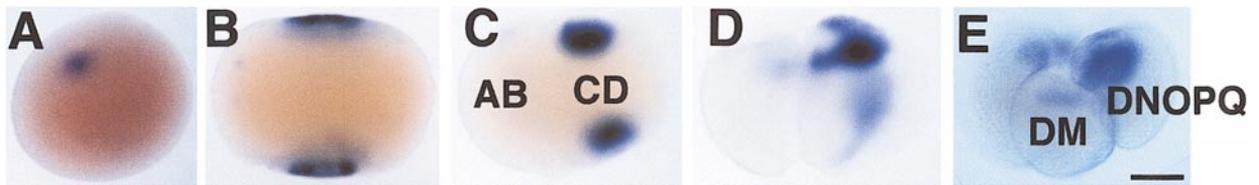
FIG. 3. Distribution and segregation of *Hro-nos* transcripts in early development, analyzed by *in situ* hybridization. Except for panel A, all embryos are shown in equatorial view, with animal pole up. (A) Obliquely animal view of early stage 1 embryo; before teloplasm formation, *Hro-nos* mRNA appears to be distributed throughout the zygote, with an additional concentration in the vicinity of the female pronucleus. (B) Late stage 1; *Hro-nos* transcripts segregate with teloplasm to the animal and vegetal poles. (C) Stage 2; *Hro-nos* mRNA is enriched in cell CD. (D) Stage 3; *Hro-nos* mRNA migrates with vegetal teloplasm to animal pole. (E) Stage 4b; *Hro-nos* mRNA is more abundant in ectodermal precursor cell (DNOPQ) than in mesodermal precursor cell (DM). Scale bar, 100 μm.

Drosophila, an ecdysozoan; *nos-1, nos-2, nos-3*; Subramaniam and Seydoux, 1999) and *Hydra* (a cnidarian; *Cnnos1, Cnnos2*; Mochizuki *et al.,* 2000). Recent studies show that *nos-1* and *nos-2* are required for PGC development and that *nos-3* controls the sperm-oocyte switch in *C. elegans* (Kraemer *et al.,* 1999; Subramaniam and Seydoux, 1999). In *Xenopus* and *Danio,* the *nos*-related mRNAs are translationally sequestered components of germ plasm (MacArthur *et al.,* 1999; Köprunner *et al.,* 2001) and *nanos1* is required for normal development of germ cells in *Danio* (Köprunner *et al.,* 2001). From those studies, it could be suggested that a *nanos*-class gene functioned in germ cell formation in the ancestral bilaterians, whereas its role in the determination of embryonic polarity arose more recently, within the evolution of the ecdysozoan lineage.

To test these ideas, we have been working to characterize the expression and function of a lophotrochozoan *nos*-class gene in the leech *H. robusta* (phylum Annelida). Our previous results are somewhat at odds with the simple interpretation presented above (Pilon and Weisblat, 1997). *Hro-nos* is present as a maternal transcript that decays rapidly during early development, but translation occurs only zygotically. HRO-NOS protein peaks at fourth cleavage and is distributed unevenly between the mesodermal and ectodermal precursor cells (DM and DNOPQ) that arise as daughters of macromere D′ at that division. This raised the possibility that *Hro-nos* mRNA might be a cortically localized ectodermal determinant that was previously postulated to be involved in the mesoderm-ectoderm fate decision (Nelson and Weisblat, 1991; Nelson and Weisblat, 1992).

Here, we have used *in situ* hybridization and Northern blots to show that *Hro-nos* transcripts are distributed uniformly throughout the early zygote and thus cannot themselves be a cortically localized determinant. We also show that *Hro-nos* is expressed zygotically during later development in 11 bilateral pairs of cell clusters in mid-body segments M8-M18. These cells arise from segmental mesoderm and it seems that a subset of them gives rise to the testisacs of the adult leech (segments M8-M13). Our results

thus support the notion that germline expression of *Hro-nos* is conserved across the three major clades of bilaterally symmetric animals, and in an animal that, by comparison with *Drosophila, Caenorhabditis,* and *Xenopus* does not segregate germline from somatic cells very early in embryonic development.

MATERIALS AND METHODS

Embryos

Helobdella robusta embryos were obtained from a laboratory breeding colony (Shankland *et al.,* 1992) or from specimens collected in a minor tributary of the American River in Sacramento, California. Embryos were cultured at 23°C in HL saline (Blair and Weisblat, 1984). The embryonic stages are as defined previously (Stent *et al.,* 1992), or in terms of the time elapsed after zygote deposition (AZD).

Lineage Tracers and Teloblast Injections

To combine *in situ* hybridization and cell lineage tracing, teloblasts, or proteloblasts in stages 6 and 7 embryos were pressure-injected with tetramethylrhodamine dextran amine (RDA, Molecular Probes Inc.) at a final concentration of 50 mg/ml in 0.2 N KCl and containing 1% fast green to monitor the injections (Weisblat *et al.,* 1980). Injected embryos were cultured to stages 9 and 10, then fixed and processed for in situ hybridization as described below. Before fixation, all embryos at mid stage 9 or beyond were relaxed in a solution of 8% ethanol in 4.8 mM NaCl, 1.2 mM KCl, 10 mM MgCl$_2$ (relaxant HL saline). Some embryos were stained with Hoechst 33258 (1 μg/ml) to visualize cell nuclei.

Selected specimens were dehydrated and embedded in epoxide embedding resin (Poly/Bed 812; Polysciences) following the manufacturer's instructions, and sectioned ($\sim$15 μm) with glass knives using a Sorvall MT2-B microtome. Sections were mounted on glass slides under coverslips in a nonfluorescing medium (Fluoromount; BDH Laboratory Supplies, Ltd.), and photographed with Nomarski optics (Zeiss Axiophot) or observed with a confocal microscope (MRC 600; Biorad) in 0.1 μm optical sections.

Developmental RT-PCR

Total RNA samples were prepared from *H. robusta* embryos at selected stages with RNA Wiz (Ambion) according to the manufacturer's instructions, using 40 embryos for each sample. The RNA samples were added to solutions containing 1X reverse transcription buffer (Gibco), 3.33 mM DTT, 0.33 mM dNTP, 3.33 μm random decamer (Ambion), and 200 U reverse transcriptase (Gibco). The mixture was incubated at 42°C for 50 min and the resultant first strand cDNA (30 μl) was stored at -20°C. PCR conditions were as described by the manufacturer of ampliTaq Polymerase (Perkin-Elmer Cetus, Norwalk, CT) except that 3 μl of cDNA template were used in 50 μl of reaction mixture.

To amplify an *Hro-nos*-specific fragment of 213 bp, a pair of PCR primers (nos-F, nos-R) was designed as follows:

nos-F: 5′-AATTGTATTATATTATTGTGCTAATTG-3′

nos-R: 5′-TTTCATCTCCAAATGTAATGACTC-3′

PCR conditions for amplifying the *Hro-nos* fragment were: 1 min at 94°C, 1 min at 58°C, and 1 min at 72°C for 5 cycles, followed by 1 min at 94°C, 1 min at 56°C, and 1 min at 72°C for 15 cycles. A 15 μl aliquot of each sample was removed after 20 cycles and the remaining material underwent 5 more cycles of amplification.

As an internal standard to adjust for differences in efficiency of RNA extraction between samples, a 488 bp fragment of 18S rRNA was amplified in parallel to each *Hro-nos* sample. For this purpose, and to attenuate the signal obtained from the abundant rRNAs, bonafide and nonextending 18S primers (competimers; Ambion) were used in a 3:7 ratio, respectively. PCR conditions for amplifying the 18S rRNA fragment were: 1 min at 94°C, 1 min at 58°C and 1 min at 72°C for 1 min for 5 cycles, followed by 1 min at 94°C, 1 min at 56°C, and 1 min at 72°C for 10 cycles. A 15 μl aliquot of each sample was removed after 15 cycles and the remaining material underwent 5 more cycles of amplification.

To quantitate PCR products, each sample was run out in a 2% agarose gel and stained with ethidium bromide. Band intensity was measured with an Alphaimager (Alpha Innotech Corp.) using Alphaease (v3.3b) program.

In Situ Hybridization

In situ hybridization was performed using digoxygenin-labeled RNA probe with some modifications of the method as described previously (Harland, 1991; Nardelli-Haefliger and Shankland, 1992). Sense and antisense probes (0.64 kb for sense, 0.55 kb for antisense) were obtained by T3 and T7 *in vitro* transcription (MEGAscript kit, Ambion) using linearized pnanosKP (Pilon and Weisblat, 1997) and subsequently hydrolyzed into shorter fragments in an alkaline solution (Cox *et al.*, 1984).

Early embryos (stages 1–8) were fixed in 4% formaldehyde in PBS (130 mM NaCl, 10 mM phosphate buffer, pH 7.4) for 1 h, then permeabilized by a 5 min incubation with 50 μg/ml proteinase K (Gibco); late embryos (stages 9–11) were fixed as described above for 30 min, then treated for 25 min in 0.5 mg/ml Pronase E (Sigma).

Hybridization was carried out overnight at 55°C in the solution containing 5X SSC, 0.1 mg/ml tRNA, 0.1 mg/ml heparin, 1X Denhart's solution (Sigma), 0.1% Tween 20, 0.1% CHAPS (Sigma), and 50% formamide for early embryos and at 59°C in a 1:1 mixture of deionized formamide and 5X SSC, 0.2 mg/ml tRNA, 0.1 mg/ml heparin, 1X Denhart's solution, 0.1% Tween 20 and 0.1% CHAPS

for late embryos. To remove unhydrolyzed probe, early embryos were treated for 1 h with 50 μg/ml RNAse A (Sigma) and late embryos for 30 min with 5 μg/ml RNAse A at 37°C. Alkaline phosphatase (AP)-conjugated anti-digoxigenin Fab fragments (Boehringer-Mannheim) were added to a dilution of 1:2000 in 1X PBS, 10% normal goat serum, 0.1% Tween 20, 0.2% Triton X 100 for early embryos and to a dilution of 1:5000 in 1X PBS, 0.1% Tween 20 for late embryos. Intact embryos were cleared by dehydration in ethanol and propylene oxide, followed by infiltration with plastic embedding medium (Poly/Bed 812; Polysciences).

Northern Blot of Dissected Embryos

To facilitate the dissection of individual blastomeres, embryos were kept in 25% propyleneglycol for 10 to 20 min (Astrow *et al.,* 1987). Northern blots were carried out as described previously (Pilon and Weisblat, 1997).

Western Blotting and Whole-Mount Immunostaining

Western blotting and whole-mount immunostaining were performed with anti-HRO-NOS antibody as described previously (Pilon and Weisblat, 1997), except that 2% nonfat milk powder (Carnation, Nestle USA, Inc.) was used instead of 5% normal goat serum for the blocking and antibody solutions in western blot experiments.

Histology

To visualize differentiated testisacs, young adult leeches were fixed in 4% formaldehyde in PBS overnight at 4°C, then rinsed, dehydrated through a series of graded alcohols to 95% and embedded in glycolmethyacrylate resin (JB-4; Polyscience, Inc.) according to the manufacturer's instructions. Embedded specimens were sectioned with glass knives on a Sorvall MT2-B microtome. Sections were mounted on glass slides and stained with freshly filtered toluidine blue (1 mg/ml 2.5% aqueous sodium carbonate, pH 11.1), or Hoechst 33258 (1 μg/ml final concentration) before cover slipping.

RESULTS

Summary of Leech Development

Relevant features of glossiphoniid leech development are summarized in Fig. 1. Briefly, cytoplasmic rearrangements before first cleavage yield animal and vegetal domains of yolk-deficient cytoplasm (teloplasm) which is segregated to the D quadrant of the 4-cell embryo by two unequal cleavages (Figs. 1A–1D) and thence to macromere D′ at the third, highly unequal cleavage (not shown). At fourth cleavage, macromere D′ divides in an obliquely equatorial plane to form DM, the mesodermal precursor and DNOPQ, the ectodermal precursor (Fig. 1E). Further cleavages of DM and DNOPQ yield additional micromeres and five bilateral pairs of teloblasts. The three remaining macromeres (in the A, B, and C quadrants) are endodermal precursor cells. Micromeres contribute nonsegmented definitive tissues to the prostomium of the adult leech and also give rise to a squamous epithelium that covers the germinal bands and

the intervening prospective dorsal territory during gastrulation (Figs. 1F–1G) (Bissen and Weisblat, 1989; Weisblat *et al.,* 1984). Teloblasts are embryonic stem cells that undergo repeated, highly unequal divisions to generate founder cells (blast cells) for segmental mesoderm and ectoderm in an anterior-to-posterior progression; four pairs of ectoteloblasts (designated N, O/P, O/P, and Q) arise from cell DNOPQ and one bilateral pair of mesoteloblasts (M) arises from cell DM.

The segmented nerve system, nephridia, epidermis, and musculature of the leech arise from anteroposteriorially arrayed columns of blast cells (blast cell bandlets) and their progeny, via intermediate structures called the germinal bands and germinal plate (Figs. 1F–1G). During stage 9, 32 segmentally iterated somites and ventral neuromeres become evident. During stages 9 through 11, these structures continue to differentiate and the midgut forms from a syncytial yolk cell (SYC), which arises by the fusion of the macromeres, teloblasts (after they cease blast cell production), and supernumerary blast cells (Figs. 1H–1I) (Isaksen *et al.,* 1999; Liu *et al.,* 1998; Nardelli-Haefliger and Shankland, 1993).

The embryonic origins of the reproductive system organs and PGCs in leech (and other annelids) is unclear. In contrast to *Drosophila* or *Caenorhabditis,* for example, there is no obvious segregation of PGC precursors in early development. Leeches are hermaphroditic, with bilaterally paired testes and ovaries. The testes connect to the exterior through segment M5 and in many species occur as segmentally iterated testisacs, linked by a sperm duct. Whether this apparently segmental organization of the testisacs is real in the sense that these organs arise from blast cells, as opposed to reflecting a secondarily imposed patterning of organs derived by migration from some other source, is unknown (Sawyer, 1986).

Maternal Hro-nos mRNA Is Broadly Distributed

Our previous studies of *Hro-nos* expression used developmental Northern and western analysis, plus immunostaining (Pilon and Weisblat, 1997). These experiments revealed that *Hro-nos* is inherited as a maternal transcript that declines to low levels during early development. HRO-NOS protein first becomes detectable during the 2-cell stage and peaks at fourth cleavage. At that time it is preferentially localized in the ectodermal precursor cell, DNOPQ.

From those results, and by analogy with contemporaneous beliefs regarding the patterns of *nos* localization and expression in *Drosophila* (Dahanukar and Wharton, 1996; Gavis *et al.,* 1996; Smibert *et al.,* 1996), we proposed that the asymmetric distribution of HRO-NOS protein might result from the localization of *Hro-nos* mRNA in the animal cortex of the zygote and early embryo. But in the absence of in situ hybridization data, this notion could not

be tested. Moreover, because transcripts and protein seemed to decline monotonically, there was no evidence for zygotic expression of *Hro-nos.* We have now succeeded in addressing these questions further.

In one series of experiments, zygotes were bisected equatorially so that pooled animal and vegetal hemispheres could be compared by Northern blot analysis (Fig. 2). By this technique, we found roughly equal amounts of the transcript in each hemisphere, contrary to the notion that *Hro-nos* mRNA is localized in the animal cortex.

This result was confirmed and extended by *in situ* hybridization (Fig. 3). In the early zygote, before the formation of teloplasm, *in situ* staining for *Hro-nos* transcripts is uniform throughout the entire embryo, except for stronger staining in the vicinity of the female pronucleus (Fig. 3A). After teloplasm has formed at the animal and vegetal poles, *Hro-nos* transcripts are seen in both pools of teloplasm (Fig. 3B). Examination of embryos stained at these stage 1 and 2 revealed that *Hro-nos* transcripts are initially located near the membrane and later spread into whole teloplasm (Figs. 3B and 3C). *Hro-nos* transcripts segregate with the bulk teloplasm into the D quadrant macromere and vegetal transcripts translocate toward the animal pole during stage 3 (Fig. 3D), as does teloplasm (Holton *et al.,* 1994). After fourth cleavage (Fig. 3E), *Hro-nos* mRNA is enriched in the teloplasm of DNOPQ (ectodermal precursor) relative to that of DM (mesodermal precursor); Northern blots comparing pools of dissected DM and DNOPQ cells indicate that DNOPQ contains twice as much *Hro-nos* mRNA as does DM (Fig. 2). Since the overall levels of *Hro-nos* are declining during this period, the difference between DM and DNOPQ could reflect either translocation or differential stability of maternal *Hro-nos* transcripts.
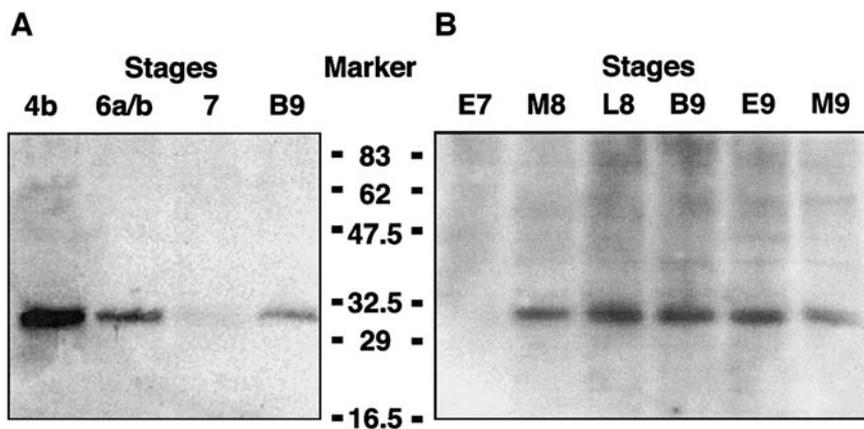
Hro-nos Is Expressed Zygotically

To test for zygotic *Hro-nos* transcription, we adapted a semi-quantitative RT-PCR technique, to avoid the need for large numbers of staged embryos for developmental Northern blot analyses. For this purpose, 18S ribosomal RNA was used as an internal standard, to control for variations in the efficiency of RNA extraction (see Materials and Methods). The results (Fig. 4) confirmed that the *Hro-nos* transcripts are present at highest levels in oocytes and decline to near background levels during stage 7, consistent with the results of *in situ* hybridization experiments (Fig. 3). But RT-PCR also revealed that *Hro-nos* levels begin to rise again during stage 8, peaking at late stage 8 and persisting through stage 10 (Fig 4). This later accumulation must represent zygotic transcription.

The existence of zygotic *Hro-nos* transcription was confirmed by in situ hybridization. Stage 7 embryos exhibit very low levels of staining, compared with stage 8 embryos processed in parallel (data not shown). These differences do not reflect penetrability differences between stages, because
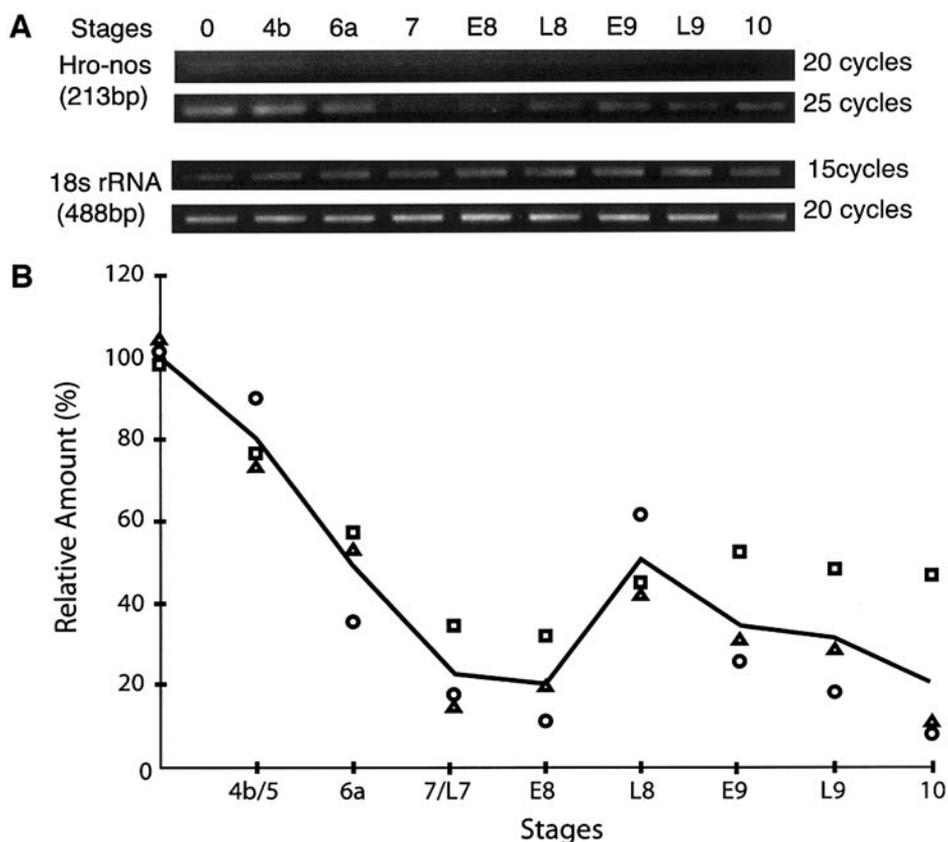
FIG. 4. RT-PCR demonstrates decline of maternal *Hro-nos,* followed by later zygotic transcription. (A) Digital images of ethidium bromide-stained agarose gels. Fragments of *Hro-nos* and 18S rRNA were amplified in separate reactions carried out in parallel. Each reaction sample contained template cDNA equivalent to 4 embryos at the stage indicated [stage 4b ~10 h AZD, stage 6a ~19 h AZD, stage 7 ~40 h AZD, early stage 8 (E8) ~64 h AZD, late stage 8 (L8) ~88 h AZD, early stage 9 (E9) ~112 h AZD, late stage 9 (L9) ~140 h AZD, stage 10 ~150 h AZD]. (B) Changes in abundance of *Hro-nos* mRNA during development, relative to oocytes (stage 0). At each stage, the intensity of the *Hro-nos* band was normalized against the 18S rRNA fragment (see Materials and Methods for details). Squares indicate the data obtained from the gels shown in (A); circles and triangles represent data obtained starting with independent sets of embryos.

FIG. 5. Western blots demonstrate zygotic HRO-NOS expression. (A) HRO-NOS protein levels decline dramatically from stage 4b to 7, correlated with the disappearance of maternal transcripts, but have increased by the beginning of stage 9 (B9 ~100 h AZD), corresponding to the onset of zygotic transcription; for this experiment each lane contains protein from 30 embryos at the stage or mixture of stages indicated. (B) Examination of additional time points reveals that, by late stage 8 (~90 h AZD), zygotic HRO-NOS expression reaches a plateau that lasts at least until mid stage 9 (M9 ~110 h AZD); for this experiment each lane contains protein from 20 embryos taken at the stage indicated.
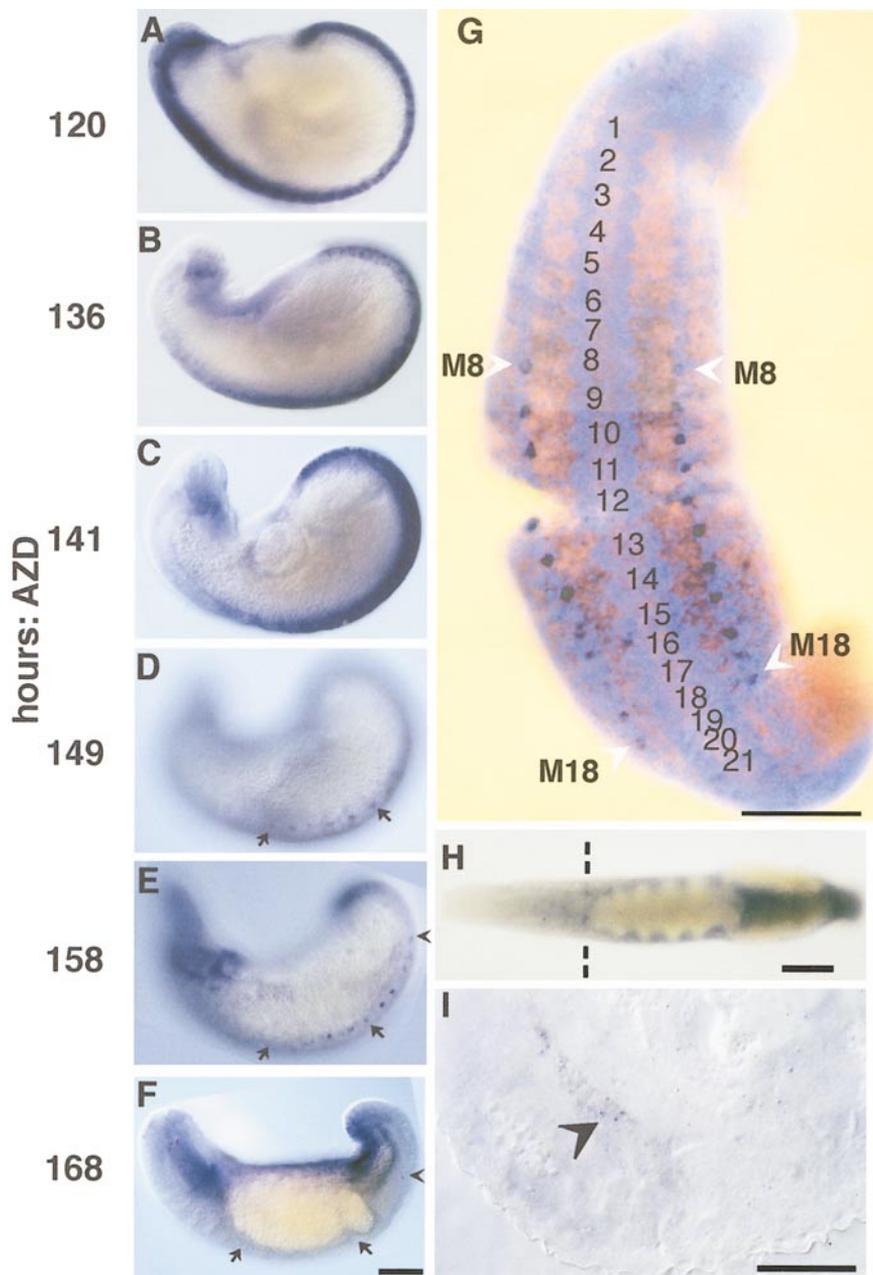
FIG. 6. Late zygotic expression of *Hro-nos* is localized to paired spots in mid-body segments M8–M18, and to the developing ovaries. (A–F) Lateral views (as in Fig. 1H, anterior to left and dorsal up) of embryos stained for *Hro-nos* mRNA by *in situ* hybridization at ages ranging from the early stage 9 (~120 h AZD) to late stage 10 (~168 h AZD). The initially widespread *Hro-nos* expression in the germinal plate declines in an anteroposterior progression, leaving a pattern of 11 paired spots, which themselves disappear later, also in an anteroposterior progression. These spots are first visible in segment M8 at ~136 h AZD, but in this figure are first obvious in panel D; in this photograph, only the first 6 spots are in focus, in segments M8–M13, where definitive testisacs arise in the adult (black arrows in panels D–F). Black arrowheads mark the *Hro-nos* spots in segment M18 in panels E and F; note that by ~168 h AZD, expression has been lost from all the anterior segments. (G) Combined brightfield and fluorescence (Hoechst 33258) image, showing a ventral view of a germinal plate dissected from an embryo hybridized for *Hro-nos* at ~155 h, then flattened under a coverslip in 100% glycerol. Anterior is up. Fluorescent nuclear staining reveals the 21 midbody ganglia (numbered). White arrowheads mark the first and last *Hro-nos* spots in segments M8 and M18. (H) Ventral view of a stage 11 embryo (~185 h AZD) stained for *Hro-nos* by *in situ* hybridization. Anterior is to the left. A pair of *Hro-nos*-positive spots lies just anterior to the midgut and the embryo was sectioned at this level, as indicated by the dotted lines. (I) DIC image, showing part of an obliquely transverse section cut from the embryo shown in panel H; dorsal is up. One arm of the ovary is visible, and is stained by the *in situ* reaction product (arrowhead). Scale bars, 100 μm for A–F; 100 μm for G; 200 μm for H; 50 μm for I.
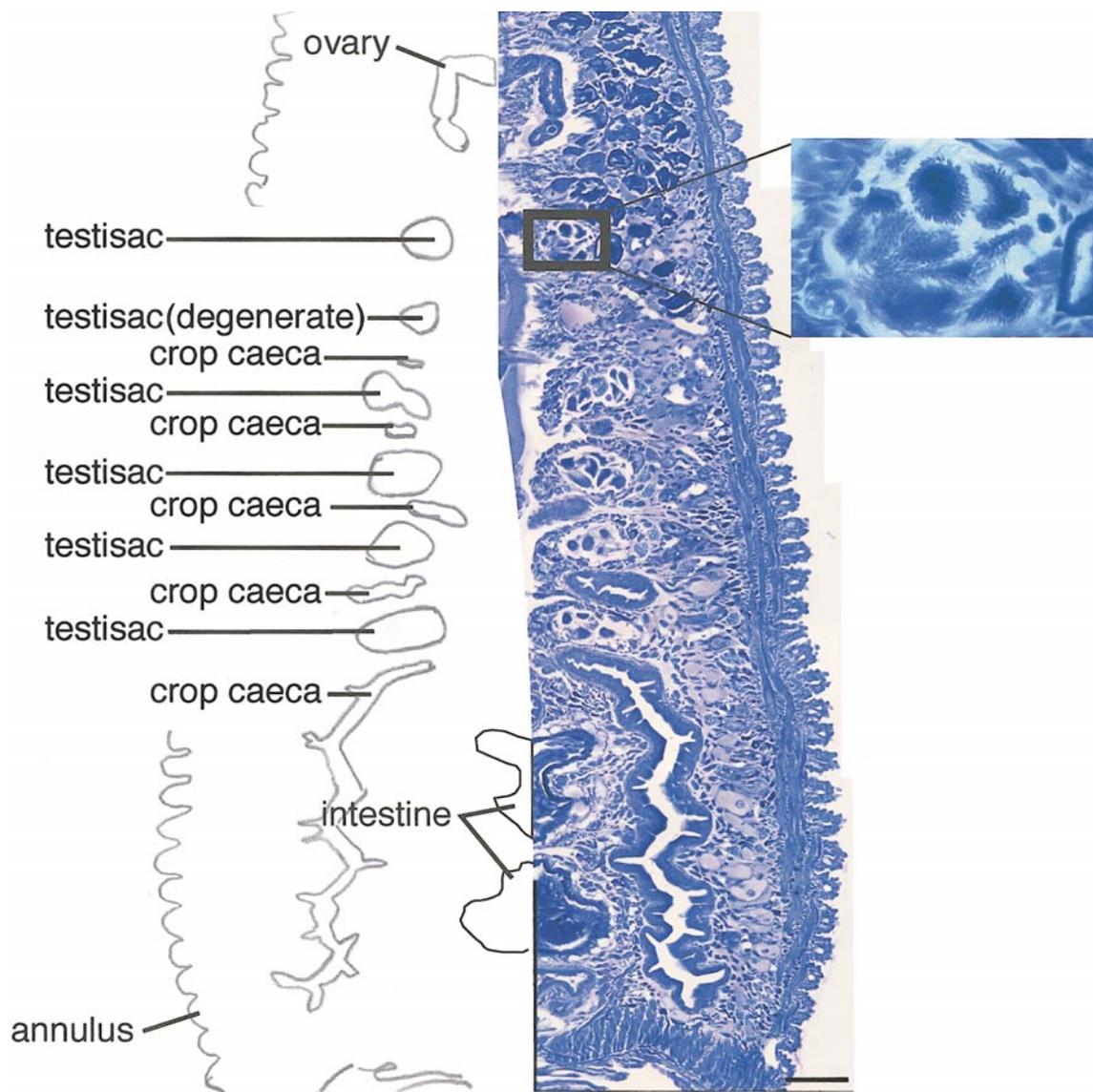
FIG. 7. Distribution of testisacs in adult *H. robusta*. Digitally montaged image showing part of a toluidine blue-stained horizontal section of an adult specimen (28 days AZD). Drawing at left is a schematized reflection across the midline of the photo at right. The characteristic morphologies of spermatogonia and spermatazoa (inset) allow the identification of five testisacs in this specimen. A lacuna is seen in the location expected for a sixth testisac and is therefore labeled as degenerate. Scale bar, 200 μm (50 μm for inset).

other probes give strong and specific staining during stage 7 (M. H. Song and DAW, unpublished observations).

Evidence for translation of the zygotic transcripts was obtained by developmental western blot (Fig. 5) and immunostaining. *In situ* hybridization and immunostaining indicate that *Hro-nos* is expressed broadly throughout the germinal bands and germinal plate, so that by the end of stage 8, *Hro-nos* expression is uniform along the length of the newly completed germinal plate (data not shown).

Late Zygotic Hro-nos Transcripts Mark Presumptive PGCs

During stages 9 and early 10, as somites and neuromeres form and differentiate, *Hro-nos* expression disappears gradually in an anteroposterior progression within the expanding germinal plate (Figs. 6A–6F). As the broadly distributed transcripts disappear, however, 11 bilaterally paired spots of *Hro-nos* expression persist, located lateral to

the segmental ganglia in segments M8-M18 (Fig. 6G). These spots, which were never seen in segments anterior or posterior to M8-M18, persist until mid stage 10 and then disappear in an anteroposterior progression. This late pattern of zygotic *Hro-nos* transcription closely resembles 11 pairs of cells described previously as presumptive gonoblasts (Bürger, 1891). In older embryos (stage 11), we observed another paired set of *Hro-nos* positive cells in segment M6 (Fig. 6H). Transverse sections reveal that these cells are located in the paired arms of the developing ovaries (Fig. 6I). These correlations suggested that *nanos*-class genes are expressed by PGCs in lophotrochozoans, as in deuterostomes and ecdysozoans (Kobayashi *et al.,* 1996; Kraemer *et al.,* 1999; MacArthur *et al.,* 1999; Subramaniam and Seydoux, 1999).

One caveat to this interpretation is that the spots of *Hro-nos* expression disappear during stage 10, long before definitive testisacs appear in the regions between the caeca of the anterior midgut. Moreover, the notion that *Hro-nos* expression marks germline precursors of prospective testisacs is problematic because *H. robusta* has only 5 to 6, rather than 11, pairs of testisacs (Fig. 7), suggesting that definitive testisacs arise from a segment-specific subset of presumptive PGCs. Intraspecies variability in the number of testisacs has been reported for other leech species (Bhatia, 1977) and in this case arises in part from the occurrence on one side or the other of what appear to be empty testisac sheaths, devoid of spermatogonia (Fig. 7).

We have previously observed sets of mesodermally derived cells in segments M8-M18 that correspond to the putative gonoblasts (Weisblat and Shankland, 1985). Therefore, to further test the correlation between presumptive gonoblasts and late zygotic *Hro-nos* expression, we examined sectioned embryos in which an M teloblast had been injected with lineage tracer (RDA) at stage 6 to 7, then processed for *Hro-nos in situ* hybridization and counterstained with Hoechst 33258 at late 9. As illustrated in Fig. 8, each spot of late zygotic *Hro-nos* expression comprises 1 to 2 cells (Figs. 8A–8C) derived from the M lineage (Figs. 8D–8F). In each cell, the *Hro-nos* transcripts are associated with cytoplasmic granules (Fig. 8C). Cells expressing *Hro-nos* lie laterally at the anterior region of each ganglion (Figs. 8B–8C), which corresponds to the site of the presumptive gonoblasts (Weisblat and Shankland, 1985).

Presumptive PGCs Arise in a Segmentally Iterated Manner from Subset of Primary m Blast Cells

Given that PGCs in segments M8-M18 arise from the M lineage, one must still distinguish between various possible origins within the M lineage. For example, one possibility is that all the PGCs arise from the M lineage before formation of the M teloblasts (via micromeres dm' or dm″), or after the formation of the teloblasts but before the production of the normal m blast cells (the first two cells produced from each M teloblast contribute a set of migratory cells that are

presumptive muscle cells of the provisional integument) (Weisblat *et al.,* 1984; C. Chi and M. Leviten, unpublished observations). Another possibility is that all ipsilateral PGCs arise from within a single segment, such as segment M5, site of the male reproductive opening, and then migrate to their final destinations (reviewed in Sawyer, 1986). Yet another possibility is that the PGCs arise in situ from the series of m blast cells that populate segments M11-M18. To address this question, we carried out *in situ* hybridization for *Hro-nos* on stage 10 embryos in which the left M teloblast had been injected with RDA at various times during stages 6 to 7. In such embryos, a boundary appears within the M lineage between unlabeled anterior segments, containing progeny of m blast cells born before the injection, and labeled posterior segments containing progeny of m blast cells born after the injection. Examining a series of such embryos showed that the PGCs arise within each segment from the m blast cell clone that contributes most of the mesodermal derivatives to the next anterior segment, consistent with the previous observations regarding the clonal origins of the "presumptive gonoblasts" (Weisblat and Shankland, 1985). For example, Fig. 9 (A and B) shows three segments (M12–M14) at the boundary between labeled and unlabeled mesoderm in one such embryo. A composite horizontal view (Fig. 9C–I) shows that, in M13 (Fig. 9F-G), the PGC contains no lineage tracer, despite the fact that other M lineage derivatives in that segment are labeled, while in segment M14 (Figs. 9H–9I), the PGC is labeled with lineage tracer.

DISCUSSION

Maternal Hro-nos Expression and Embryonic Polarity

The results presented here show that in the leech *H. robusta*: 1) maternal *Hro-nos* transcripts are uniformly distributed in the early zygote; 2) they become concentrated into teloplasm as it forms at the animal and vegetal poles prior to first cleavage (as do the bulk of maternal polyadenylated mRNAs; Holton *et al.,* 1994); 3) they then segregate with teloplasm into D quadrant cells during early cleavage, and; 4) by stage 4b, they are at higher levels in the ectodermal precursor cell DNOPQ than in the mesodermal precursor cell DM. These results contradict the model that cortically localized *Hro-nos* mRNA accounts for the previously described differential of HRO-NOS protein expression at stage 4b (higher in DNOPQ than in DM; Pilon and Weisblat, 1997). From our present results, differences in RNA levels alone could account for the differences in HRO-NOS protein between these two cells, or, by homology with analyses of the *nanos* syntagma in *Drosophila* and vertebrates (see below), a gradient could form by localized translation, under the control of determinants at the animal side of the embryo.

In *Drosophila,* maternal *nanos* mRNA was originally thought to be localized to the posterior pole (Gavis and

Lehmannn, 1992; Wang *et al.,* 1994). But it is now known that most of the maternal *nanos* transcripts in *Drosophila* are distributed throughout the zygote (Bersten and Gavis, 1999) and that formation of the NANOS gradient in *Drosophila* reflects a repression of *nanos* translation in the bulk cytoplasm by RNA binding proteins like SMAUG (Clark *et al.,* 2000; Smibert *et al.,* 1999), with localized derepression of translation at the posterior pole cortically localized products of other genes such as *vasa* and *tudor* (Wang *et al.,* 1994). Whether *Hro-nos* translation is similarly controlled remains to be determined; differential protein stability could also contribute to the differences in HRO-NOS levels between DM and DNOPQ in *Helobdella.* Moreover, it is not known if the differences in HRO-NOS levels are part of the mechanism for specifying distinct ectodermal and mesodermal fates for these two cells. But if *Hro-nos* is translationally regulated, and if HRO-NOS levels play a role in the DM-DNOPQ fate decision, then cortically localized factors required for translation of *Hro-nos* mRNAs in teloplasm could be the cortically located ectodermal determinants postulated from previous studies (Nelson and Weisblat, 1991; Nelson and Weisblat, 1992).

In any event, we now know that representatives of both the major groups of protostomes (*Helobdella,* a Lophotrochozoan; and *Drosophila,* an Ecdysozoan) generate early gradients of NOS-class protein, and that such gradients have not been reported for deuterostome embryos. This suggests the possibility that the use of *nanos*-class genes in establishing embryonic polarity is an ancestral feature of the protostomes. But *nanos* homologs play no such role in *Caenorhabditis,* so the question of whether this similarity between *Drosophila* and *Helobdella* represents evolutionary conservation or convergence requires the study of other protostome species.

Early Zygotic Hro-nos Expression

Our results also provide the first evidence that *Hro-nos* is transcribed zygotically. This zygotic expression is widespread within the germinal bands and germinal plate during stage 8 and early stage 9 and then declines in a fairly uniform anteroposterior progression (with the clear exception of the 11 paired sets of cells as discussed in the following section).

In *Drosophila,* NANOS and PUMILIO function as co-repressors to inhibit the translation of *hunchback* mRNA (Irish *et al.,* 1989; Sonoda and Wharton, 1999). In leech, it was reported that RNA of a *hunchback* ortholog, *lzf2,* is expressed uniformly along the length of the segmental truck in both the ectodermal and mesodermal tissues (Savage and Shankland, 1996), but that LZF2 protein is not expressed in germinal plate, but rather in adjacent cells of the provisional integument (Iwasa *et al.,* 2000). From the fact HRO-NOS protein is expressed in the growing germinal plate and LZF2 protein is not, one possible role of HRO-

NOS protein in germinal plate might be to inhibit the translation of *lzf2,* but this remains to be determined.
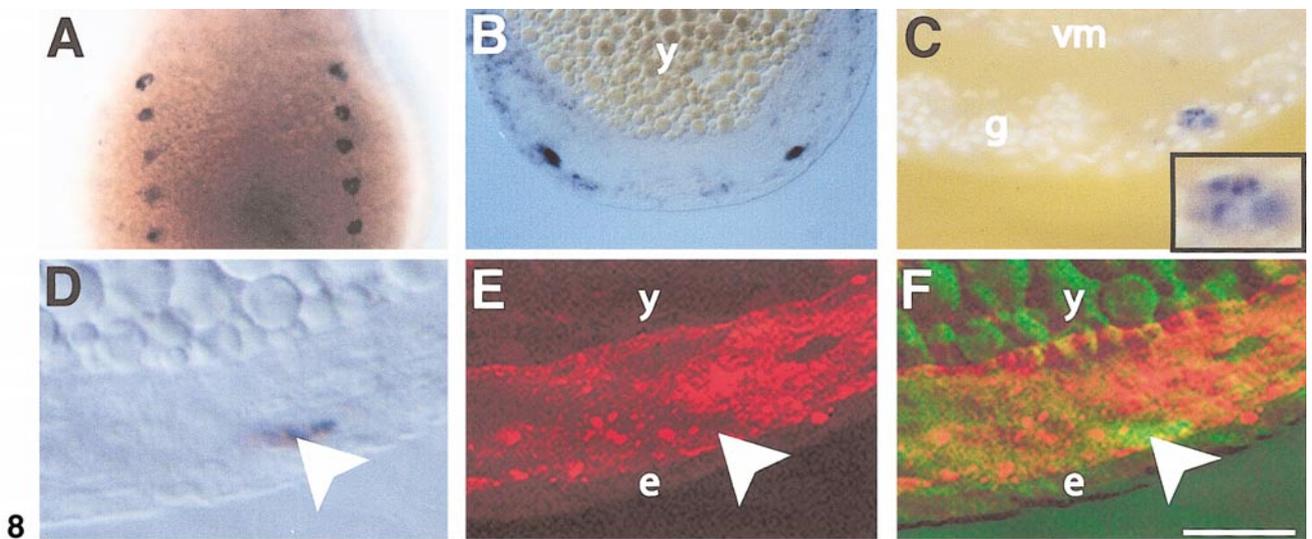
Late Zygotic Hro-nos Expression and Gonad Formation in Leeches

During late stage 9, expression of *Hro-nos* declines throughout the germinal plate, except for 11 paired sets of cells, in segments M8-M18, in which expression persists until late stage 10. In these cells, the *Hro-nos* transcripts occur in a granular distribution in the cyctoplasm, as has been reported for the germ plasms of other organisms (Mahowald, 1971; Williams and Smith, 1971; Eddy, 1975; Strome and Wood, 1982). These 11 sets of cells are presumably the same as those that had been previously proposed as gonoblasts (PGCs) by Bürger (1891) and had been shown to arise from the M teloblasts (Weisblat and Shankland, 1985). They are more accurately to be regarded as "pre-PGCs", because only 4 to 6 pairs of testisacs, located in segments M8–M13, arise from the original 11 sets of cells on each side. Whether cell-intrinsic or position-dependent cues are responsible for this selection remains to be determined. We have also observed paired sets of cells expressing *Hro-nos* in segment M6, that we propose to be the PGCs for the ovaries of these hermaphroditic annelids.

In all leeches, the male and female genital pores are associated with segments M5 and M6, respectively, and it has previously been demonstrated (Gleizer and Stent, 1993) that the m blast cells contributing to segments M5 and M6 in glossiphoniid leeches give rise to male and female genital primordia, respectively. Our present results indicate that the male genital primordia must contribute only somatic tissues to the male reproductive tract, because the male PGCs arise from the m blast cells contributing to more posterior segments. By contrast, for the female reproductive tract, both somatic and germ cells may arise from the same m blast cell.

We have also shown that these pre-PGCs (as defined by *Hro-nos* expression) arise in a segmentally iterated manner from the late M lineage, contrast to the situation in *Xenopus, Danio, Drosophila,* and *Caenorhabditis,* where PGCs are established early in development on the basis of germ plasm inheritance. In *Helobdella,* each of 11 successive m blast cells on each side generates a set of pre-PGCs. These m blast cells arise after more than 20 rounds of zygotic mitosis, and because each m blast cell contributes a diverse set of cell types including muscle, nephridia, neurons, and connective tissue, the pre-PGCs must arise even later in the cell lineage.

As reviewed by Sawyer (1986), the testisacs in most leeches extend posteriorly usually as discrete, segmentally iterated sacs connected by a sperm duct, as in *Helobdella.* The exact number of testisacs varies between species and to a lesser degree within species. In the strain of *H. robusta* used for this work, we found 4 to 6 testisacs on each side, and similar values are obtained for other species in this
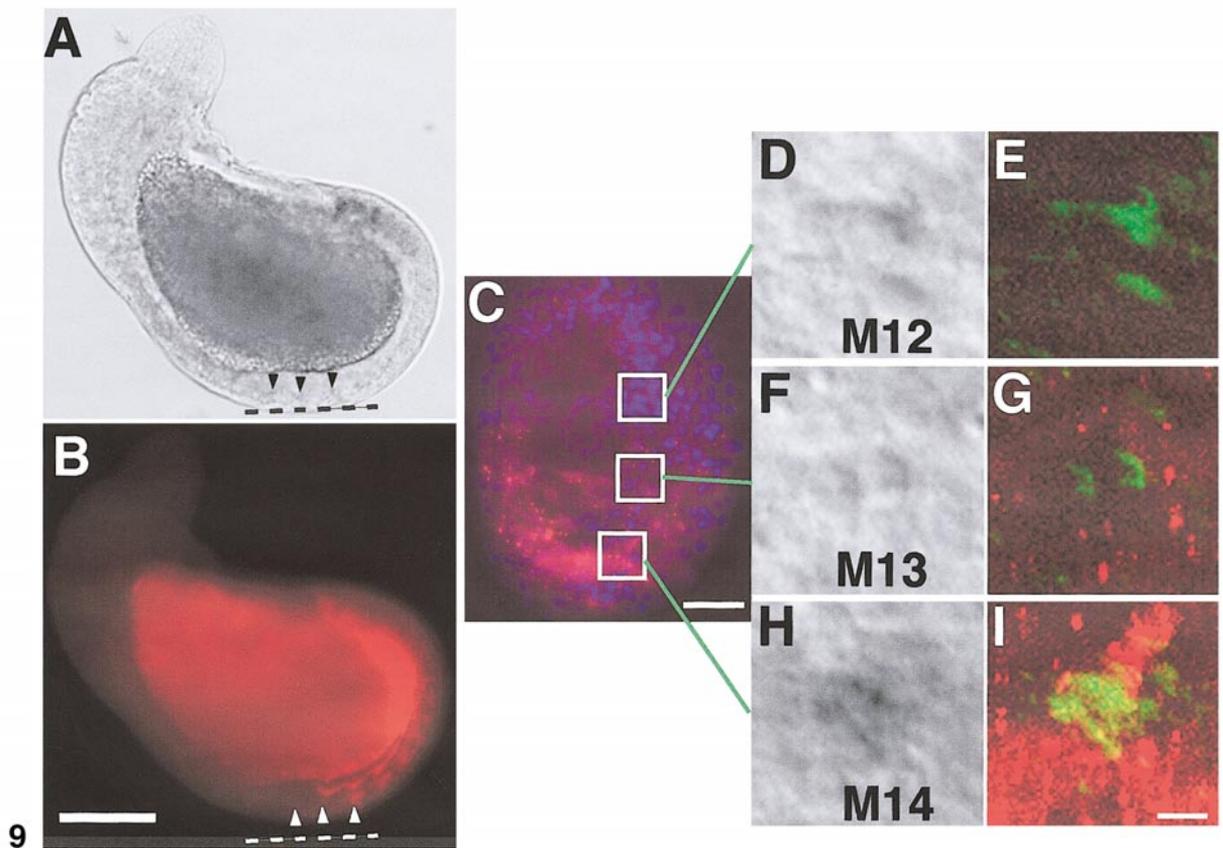
FIG. 8. Paired spots of late zygotic *Hro-nos* expression arise from the mesodermal lineage. (A) Ventral view (anterior is up) of a late stage 9 embryo, showing the anterior-most 5 pairs of late zygotic *Hro-nos*. (B) Brightfield image of a transverse section through a similar embryo, showing one pair of spots, just inside the body wall; yolk platelets (y) mark the prospective midgut. (C) Combined brightfield and fluorescence (Hoechst 33258) image of a similar section, showing the position of the *Hro-nos* spot relative to the segmental ganglion (g) and the visceral mesoderm (vm). In this section, one nucleus is visibly surrounded by the in situ reaction product; adjacent sections revealed another cell within the same *Hro-nos* spot (not shown). Higher magnification (inset) reveals a granular distribution of transcripts in the cell expressing *Hro-nos*. (D) Brightfield and (E) pseudo-colored confocal images of a transverse section showing an *Hro-nos* spot (white arrowhead) from an embryo in which an M teloblast had been injected with RDA at stage 6. In panel E, RDA-labeled mesoderm (red) occupies the space between the yolk (y) and the body wall epidermis (e). (F) Pseudo-colored, digital superimposition of panels D and E, showing that the *Hro-nos* (green) arises within the mesodermal layer. Scale bar, 125 μm in A; 110 μm in B; 60 μm in C (25 μm for inset); 50 μm in D–F.

genus (Gullo, 1995; our unpublished observations). Other species have more, including 10 pairs in *Haemopis sanguisuga,* 9–10 in *Hirudo medicinalis,* and 11 (occasionally 12) in *Hirudinaria granulosa* (Bhatia, 1977). We find no reports of greater numbers of testisacs in any other leech, and the 11 pairs of testisacs arising normally in *Hirudinaria* fall in the same segments as the 11 pairs of pre-PGCs in *Helobdella.* Thus, the formation of 11 paired sets of pre-PGCs may be ancestral among leeches.

Comparisons with Oligochaetes and Other Animals

Clitellate annelids are a clade comprising oligochaetes and leeches. All clitellate species are hermaphroditic, but until recently, little has been known about their germ cell formation. It had been reported that PGCs arise as products of the pair of cells produced at the first cell divisions by the M teloblasts in tubificid and enchytraeid oligochaetes (reviewed by Anderson, 1973), a finding that is at odds with what we now know about the origins of PGCs and somatic gonadal tissues in leech (see preceding section). A more recent cell lineage analysis in *Tubifex* revealed prominent pairs of M teloblast-derived cells that appear to arise in situ within the reproductive segments, segments X and XI, and are identified as male and female PGCs, respectively (Goto *et al.,* 1999), although the possibility that these presumptive PGCs migrate to segments X and XI from elsewhere in the mesoderm was not addressed.

Our finding that PGCs do not segregate from other lineages until more than 20 rounds of zygotic mitosis suggests that in contrast to *Drosophila, Caenorhabditis,* or *Xenopus* (reviewed in Houston and King, 2000; reviewed in Ikenishi, 1998; see also Kemphues and Strome, 1997; see also Mahowald, 1962), leeches contain no germ plasm that uniquely specifies one set of cells to be set aside as the exclusive germ cell lineage early in embryogenesis. Further evidence for this conclusion comes from observations that some oligochaete species can regenerate intact worms, complete with gonads, from body fragments that do not contain gonads (reviewed in Stephenson, 1930). For example, it was found that in the oligochaete *Criodilus lacuum,* which normally contains two pairs of testes and one pair of ovaries, the regeneration of gonads is irregular with respect to both location and number of gonads regenerated, up to a total of 12 pairs, similar to what we propose as the ancestral number for leech pre-PGCs. Whether this similarity reflects some feature of the ancestral clitellate remains to be determined.

ACKNOWLEDGMENTS

REFERENCES

Anderson, D. T. (1973). Embryology and Physiology in Annelids and Arthropods. Oxford, UK: Pergamon Press.

Astrow, S. H., Holton, B., and Weisblat, D. A. (1987). Centrifugation redistributes factors determining cleavage patterns in leech embryos. *Dev. Biol.* **120,** 270–283.

Bersten, S. E., and Gavis, E. R. (1999). Role for mRNA localization in translational activation but not spatial restriction of *nanos* RNA. *Development* **126,** 659–669.

Bhatia, M. L. (1977). Memoirs on Indian animal types. Delhi, India: Emkay Publications.

Bissen, S. T., and Weisblat, D. A. (1989). The durations and compositions of cell cycles in embryos of the leech, *Helobdella triserialis. Development* **106,** 105–118.

Blair, S. S., and Weisblat, D. A. (1984). Cell interactions in the developing epidermis of the leech *Helobdella triserialis. Dev. Biol.* **101,** 318–325.

Bürger, O. (1891). Beitrage zur Entwicklungsgeschichte der Hirudineen. Zur Embryologie von Nephelis. *Zool. JB. Anat. Ont.* **4,** 697–783.

Clark, I. E., Wyckoff, D., and Gavis, E. R. (2000). Synthesis of the posterior determinant *nanos* is spatially restricted by a novel

FIG. 9. *Hro-nos* spots arise in a segmentally iterated manner from m blast cells. (A) and (B) Brightfield and fluorescence images, respectively, showing lateral views (anterior to left, dorsal is up) of an embryo in which an M teloblast had been injected with RDA at stage 7 (39 h AZD), well after the onset of blast cell production, to generate a boundary between labeled and unlabeled segments (Zackson, 1982) that would fall in the mid body region. The embryo was then cultured to mid stage 9 (~140 h AZD) and processed for *Hro-nos in situ* hybridization. Black arrowheads in panel A indicate *Hro-nos* spots in segments M12–M14. White arrowheads in panel B indicate the same three segments, which overlap the boundary between RDA-labeled and unlabeled segments. Note that, because adjacent m blast cell clones interdigitate along the anteroposterior axis, not all the M teloblast derivatives in segment M13 are labeled. This embryo was sectioned in a roughly horizontal plane, as indicated by the dotted lines. (C) Fluorescence image, showing nuclei (Hoechst 33258, blue) and lineage tracer (RDA, red) of a section that includes parts of the *Hro-nos* spots in segments M12–M14 on the RDA-labeled side of the embryo (anterior is up; ventral midline to right). *Hro-nos*-positive cells lie in the areas enclosed by white boxes in each segment, as revealed by the corresponding brightfield images in panels D, F, and H. Combined brightfield and fluorescence images of the same fields (E, G, and I, respectively; hybridization signal is pseudo-colored green), reveal that the cells expressing *Hro-nos* in segment M14 also contain lineage tracer, while those in segments M12 and M13 do not. Scale bars, 100 μm in A and B; 20 μm in C; 4 μm in D–I.

cotranslational regulatory mechanism. *Curr. Biol.* **10**. 1311–1314.

Cox, K. H., DeLeon, D. V., Angerer, L. M., and Angerer, R. C. (1984). Detection of mRNAs in sea urchin embryos by in situ hybridization using asymmetirc RNA probes. *Dev. Biol.* **101**, 485–502.

Dahanukar, A., and Wharton, R. P. (1996). The *nanos* gradient in *Drosophila* embryos is generated by translational regulation. *Genes Dev.* **10**, 2610–2620.

Deshpande, G., Calhoun, G., Yanowitz, J. L., and Schedl, P. D. (1999). Novel functions of *nanos* in downregulating mitosis and transcription during the development of the *Drosophila* germline. *Cell* **99**, 217–281.

Eddy, E. M. (1975). Germ plasm and the differentiation of the germ cell line. *Int. Rev. Cytol.* **43**, 229–280.

Forbes, A., and Lehmann, R. (1998). *Nanos* and *pumilio* have critical roles in the development and function of *Drosophila* germline stem cells. *Development* **125**, 679–690.

Gavis, E. R., and Lehmann, R. (1992). Localization of *nanos* RNA controls embryonic polarity. *Cell* **71**, 301–313.

Gavis, E. R., Lunsford, L., Bergsten, S. E., and Lehmann, R. (1996). A conserved 90 nucleotide element mediates translational repression of *nanos* RNA. *Development* **122**, 2791–2800.

Gleizer, L., and Stent, G. S. (1993). Developmental origin of segmental identity in the leech mesoderm. *Development* **117**, 177–189.

Goto, A., Kitamura, K., Arai, A., and Shimizu, T. (1999). Cell fate analysis of teloblasts in the *Tubifex* embryo by intracellular injection of HRP. *Develop. Growth Differ.* **41**, 703–713.

Gullo, B. S. (1995). Microanatomy of the male gonads and ducts of *Helobdella triserialis*. *Neotropica* **41**, 67–75.

Harland, R. M. (1991). In situ hybridiazation: An improved wholemount method for *Xenopus* embryos. *Methods Cell Biol.* **36**, 685–695.

Holton, B., Wedeen, C. J., Astrow, S. H., and Weisblat, D. A. (1994). Localization of polyadenylated RNAs during teloplasm formation and cleavage in leech embryos. *Roux's Arch. Dev. Biol.* **204**, 46–53.

Houston, D. W., and King, M. L. (2000). Germ plasm and molecular determinants of germ cell fate. *Curr. Top. Dev. Biol.* **50**, 155–181.

Ikenishi, K. (1998). Germ plasm in *Caenorhabditis elegans, Drosophila* and *Xenopus. Dev. Growth Differ.* **40**, 1–10.

Irish, V., Lehmann, R., and Akam, M. (1989). The *Drosophila* posterior-group gene *nanos* functions by repressing *hunchback* activity. *Nature* **338**, 646–648.

Isaksen, D. E., Liu, N. L., and Weisblat, D. A. (1999). Inductive regulation of cell fusion in leech. *Development* **126**, 3381–3390.

Iwasa, J. H., Suver, D. W., and Savage, R. M. (2000). The leech *hunchback* protein is expressed in the epithelim and CNS but not in the segmental precursor lineage. *Dev. Genes Evol.* **210**, 277–288.

Kemphues, K., and Strome, S. (1997). Fertilization and establishment of polarity in the embryo. In "*C. elegans II*" (T. B. D. Riddle, B. Meyer, and J. Priess, Eds.), pp. 335–359. Cold Spring Harbor, NY: Cold Spring Harbor Press.

Kobayashi, S., Yamada, M., Asaoka, M., and Kitamura, T. (1996). Essential role of the posterior morphogen *nanos* for germline development in *Drosophila. Nature* **380**, 708–711.

Köprunner, M., Thisse, C., Thisse, B., and Raz, E. (2001). A zebrafish *nanos*-related gene is essential for the development of primordial germ cells. *Genes Dev.* **15**, 2877–2885.

Kraemer, B., Crittenden, S., Gallegos, M., Moulder, G., Barstead, R., Kimble, J., and Wickens, M. (1999). NANOS-3 and FBF proteins physically interact to control the sperm-oocyte switch in *Caenorhabditis elegans. Curr. Biol.* **9**, 1009–1018.

Liu, N.-J. L., Isaksen, D. E., Smith, C. M., and Weisblat, D. A. (1998). Movements and stepwise cell fusion of endodermal precursor cells in leech. *Dev. Genes Evol.* **208**, 117–127.

MacArthur, H., Bubunenko, M., Houston, D. W., and King, M. L. (1999). *Xcat2* RNA is a translationally sequestered germ plasm component in *Xenopus. Mech. Dev.* **84**, 75–88.

Mahowald, A. P. (1962). Fine structure of pole cells and polar granules in *Drosophila melanogaster. J. Exp. Zool.* **151**, 210–205.

Mahowald, A. P. (1971). Polar granules of *Drosophila*. 3. The continuity of polar granules during the life cycle of *Drosophila. J. Exp. Zool.* **176**, 329–343.

Mochizuki, K., Sano, H., Kobayashi, S., Nishimiya-Fujisawa, C., and Fujisawa, T. (2000). Expression and evolutionary conservation of *nanos*-related genes in *Hydra. Dev. Genes Evol.* **210**, 591–602.

Mosquera, L., Forristall, C., Zhou, Y., and King, M. L. (1993). A mRNA localized to the vegetal cortex of *Xenopus* oocytes encodes a protein with a *nanos*-like zinc finger domain. *Development* **117**, 377–386.

Murata, Y., and Wharton, R. P. (1995). Binding of *pumilio* to maternal *hunchback* mRNA is required for posterior patterning in *Drosophila* embryos. *Cell* **80**, 747–756.

Nardelli-Haefliger, D., and Shankland, M. (1992). *Lox2*, a putative leech segment identity gene, is expressed in the same segmental domain in different stem cell lineages. *Development* **116**, 697–710.

Nardelli-Haefliger, D., and Shankland, M. (1993). *Lox10*, a member of the *NK-2* homeobox gene class, is expressed in a segmental pattern in the cephalic nervous system of the leech *Helobdella. Development* **118**, 877–892.

Nelson, B. H., and Weisblat, D. A. (1991). Conversion of ectoderm to mesoderm by cytoplasmic extrusion in leech embryos. *Science* **253**, 435–438.

Nelson, B. H., and Weisblat, D. A. (1992). Cytoplasmic and cortical determinants interact to specify ectoderm and mesoderm in the leech embryo. *Development* **115**, 103–115.

Parisi, M., and Lin, H. (2000). Translational repression: a duet of *nanos* and *pumilio. Curr. Biol.* **10**, R81–83.

Pilon, M., and Welsblat, D. A. (1997). A *nanos* homolog in leech. *Development* **124**, 1771–1780.

Savage, R. M., and Shankland, M. (1996). Identification and characterization of a *hunchback* orthologue, *lzf2*, and its expression during leech embryogenesis. *Dev. Biol.* **175**, 205–217.

Sawyer, R. T. (1986). Clitellate reproduction and phylogenetic affinities. Oxford, UK: Clarendon Press.

Shankland, M., Bissen, S. T., and Weisblat, D. A. (1992). Description of the California leech *Helobdella robusta* sp. nov., and comparison to *H. triserialis* on the basis of morphology, embryology, and experimental breeding. *Can. J. Zool.* **70**, 1258–1263.

Smibert, C. A., Lie, Y. S., Shillinglaw, W., Henzel, W. J., and Macdonald, P. M. (1999). Smaug, a novel and conserved protein, contributes to repression of *nanos* mRNA translation in vitro. *RNA* **5**, 1535–1547.

Smibert, C. A., Wilson, J. E., Kerr, K., and Macdonald, P. M. (1996).

SMAUG protein represses translation of unlocalized *nanos* mRNA in the *Drosophila* embryo. *Genes Dev.* **10,** 2600–2609.

Sonoda, J., and Wharton, R. P. (1999). Recruitment of NANOS to *hunchback* mRNA by PUMILIO. *Genes Dev.* **13,** 2704–2712.

Stent, G. S., Kristan, W. B. J., Torrence, S. A., French, K. A., and Weisblat, D. A. (1992). Development of the leech nervous system. *Int. J. Neurol.* **33,** 109–193.

Stephenson, J. (1930). Regeneration. In "The Oligochaeta", pp. 555–600. Oxford, UK.: Clarendon Press.

Strome, S., and Wood, W. B. (1982). Immunofluorescence visualization of germ-line-specific cytoplasmic granules in embryos, larvae, and adults of *Caenorhabditis elegans. Proc. Natl. Acad. Sci. USA* **79,** 1558–1562.

Subramaniam, K., and Seydoux, G. (1999). *Nos-1* and *nos-2,* two genes related to *Drosophila* nanos, regulate primordial germ cell development and survival in *Caenorhadbitis elegans. Development* **126,** 4861–4871.

Wang, C., Dickinson, L. K., and Lehmann, R. (1994). Genetics of *nanos* localization in *Drosophila. Dev. Dyn.* **199,** 103–115.

Weisblat, D. A., Kim, S. Y., and Stent, G. S. (1984). Embryonic origins of cells in the leech *Helobdella triserialis. Dev. Biol.* **104,** 65–85.

Weisblat, D. A., and Shankland, M. (1985). Cell lineage and segmentation in the leech. *Philos. Trans. R. Soc. Lond. B. Biol. Sci.* **313,** 39–56.

Weisblat, D. A., Zackson, S. L., Blair, S. S., and Young, J. D. (1980). Cell lineage analysis by intracellular injection of fluorescent tracers. *Science* **209,** 1538–1541.

Williams, M. A., and Smith, L. D. (1971). Ultrastructure of the "germinal plasm" during maturation and early cleavage in *Rana pipiens. Dev. Biol.* **25,** 568–580.

Zackson, S. L. (1982). Cell clones and segmentation in leech development. *Cell* **31,** 761–770.